# EXPERIMENTAL STUDY ON TRANSONIC SHOCK WAVE / TURBULENT BOUNDARY LAYER INTERACTIONS AND SEPARATION INSTABILITIES. SUCTION AND REYNOLDS NUMBER EFFECTS.

**D. CARUANA**, CERT-ONERA, Aerothermodynamics Department, Toulouse, France.
**C. BULGUBURE**, Dassault Aviation, Mérignac, France
**A. MIGNOSI**, CERT-ONERA, Aerothermodynamics Department, Toulouse, France

## Abstract

In transonic flow, the shock wave / boundary layer interaction and flow separation may have important influence on the aerodynamic behaviour of the aircraft. Experimental studies in this field have been conducted by CERT-ONERA in co-operation with Dassault Aviation with the financial support of STPA. Aerodynamic wind tunnel studies on stiff 2D airfoil have been performed to analyse the effects of the Reynolds number, the boundary layer suction upstream of the shock and the downstream displacement of the transition tripping on appearance of unsteadiness resulting of shock wave / boundary layer interaction and flow separation.

The OALT25 laminar airfoil has been selected for these tests. The experiments were achieved in transonic, cryogenic, pressurised T2 wind tunnel, which is equipped with self-adaptive top and bottom walls. High Reynolds numbers were obtained by using high pressure and low temperature flow.

This paper describes the measurements carried out and illustrates the most interesting results.

## Introduction

The transonic flows are often crossed by shock waves induced by the gradient modification of a wall or by a contra-pressure constraining the flow to become subsonic. These waves are in contact with the boundary layer. That induces a complex phenomenon of interaction with flow separation and instabilities.

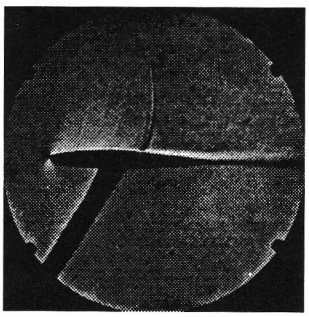

fig.1 : M0=0,78 ; $\alpha = 2°$

For example, the figure 1, N.C. Lambourne 1958 (1), shows the visualisation by Schlieren of an airfoil in transonic flow with flow separation downstream the shock. Unsteadiness and oscillating flows can appear in such a configuration.

The objectives of these tests, performed in turbulent two-dimensional flow with transition fixing, are essentially:

- Reynolds number effect study,
- study of the effect of the boundary layer suction upstream of the shock,
- study of the effect of the displacement of the transition tripping,

on appearance of unsteadiness resulting of shock wave / boundary layer interaction and flow separation.

The increase in the shock wave intensity is performed by variation of the angle of attack (0° to 2,75°) and of the Mach number (0,72 to 0,80). The variation of the boundary layer parameters conditions is performed by chord Reynolds number increase (6 million to 20 million), by boundary layer suction (average suction speed, Vasp, from 0 to 3,6 m/s) or by downstream displacement of the transition tripping (position, x/cT, from 5% to 40% of chord).

The evolution of the shock wave / boundary layer interaction and flow separation is analysed by the following parameters :

-local Mach number distributions of the model,
-boundary layer parameters,
-shock position,
-separation zones (oil flow visualisations and trailing edge pressure coefficients, Kpbf),
-unsteady wall pressure fluctuations (analysis of signal fluctuations and signal spectra).

After a presentation of the instrumentation and acquisition systems, we will illustrate the most interesting results.

## Notations

| | |
|---|---|
| u' | x axis velocity fluctuation |
| U | flow velocity |
| M0, M | flow Mach number |
| Pt, Pi | total pressure |
| Tt, Ti | total temperature |
| Rc, Re | chord Reynolds number |
| Ps, P | static pressure |
| P' | pressure fluctuation |
| Kpbf | trailing edge pressure coefficient |

Ue velocity at the edge of the boundary layer

ρ density

δ1 displacement thickness :

$$\delta 1 = \int_0^{\delta} (1 - \frac{\rho U}{\rho e Ue}) \, dy$$

θ momentum thickness :

$$\theta = \int_0^{\delta} \frac{\rho U}{\rho e Ue} (1 - \frac{U}{Ue}) \, dy$$

Hi incompressible shape parameter

$$Hi = \frac{\delta 1i}{\theta i} \text{ with } \quad \delta 1i = \int_0^{\delta} (1 - \frac{U}{Ue}) \, dy$$

$$\theta i = \int_0^{\delta} \frac{U}{Ue} (1 - \frac{U}{Ue}) \, dy$$

α model angle of attack

Vasp suction velocity

RMS root mean square of the pressure fluctuation p'

$\sqrt{\overline{p'^2}}$ (between 5 and 1000 Hz)

Ml local Mach number of the model

x/c chord position

xT, x/cT chord position of the transition fixing

E energy

f frequency

## Experimental details

### The T2 wind tunnel

Tests are carried out in the transonic T2 wind tunnel of CERT ONERA (2) (figure 2). This facility operates by runs of one to two minutes.

- **Transonic**
- **Pressurised**
- **Self - Adaptive Walls**
- **Cryogenic**

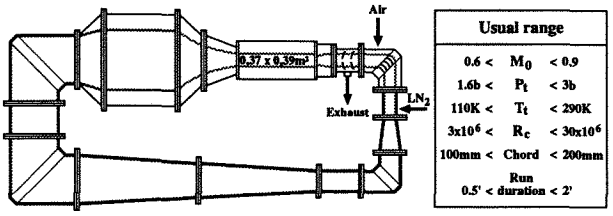


fig. 2 : T2 wind tunnel

The T2 wind tunnel is a closed circuit, in which the flow is driven by injection of pressurised dry air. Sprayed liquid nitrogen cools down the flow and the control of the temperature of the mixture "air-gaseous nitrogen" allows to adjust the Reynolds number of the test in a large range.

The test section is 0,37 m high, 0,39 m wide and 1,4 m long. It is equipped with top and bottom flexible walls. An adaptation strategy 2D or 3D according to the model geometry provides in real time the top and bottom wall shapes which cancel (for 2D flows) or minimise (for 3D flows) the wall interference. The wall adaptation is performed iteratively during the first part of the run, before the data acquisition.

A sonic throat located downstream of the test section allows to control the free stream Mach number.

The turbulence level in the T2 wind tunnel test section is about $\sqrt{u'^2} / U = 0,15\%$.

During the run, test parameters (stagnation pressure, stagnation temperature and Mach number) are controlled by a regulation system connected to a computer.

### Models and suction system

Two models of OALT25 airfoil, designed by the Aerodynamics Direction of ONERA. and manufactured by ONERA/IMFL, were used (chord : 250 mm).

The first one, OALT25-A (figure 3), was designed for cryogenic tests. This model can be cooled. To decrease the model temperature in order to reach rapidly the thermal equilibrium during the starting phase of the cryogenic tests, the model was realised with thin skin of 3 mm thick.

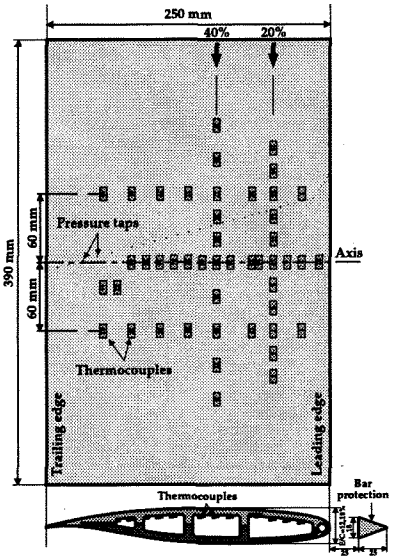


fig. 3 : Model and equipment - OALT25-A

The second one, OALT25-B (figure 4), was designed for boundary layer suction tests. This model cannot be cooled. The "suction part" can be replaced by the "smooth part". With the "smooth part", comparisons between the two models could be made. The downstream displacement of the transition tripping was also tested with the second model.

The boundary layer suction device is located upstream of the shock wave between 20% and 32% of chord. The permeability is performed by a perforated titanium sheet of 0,9 mm thick. The holes are normal to the surface. The holes diameter is 0,1 mm and the

porosity coefficient is about 4%. There is only one chamber which is connected to two pipes (equivalent diameter of 18 mm) inside the model. The adjustment and the control of the suction flow are performed by sluice-gates and sonic throats. The sonic throats measurements are realised by static and total pressure taps. The suction velocities are fixed between the minimum suction velocity without recirculation (0,2 m/s) and the maximum realisable suction velocity (3,6 m/s for a Mach number of 0,78). Some static pressure taps are located inside the chamber for control of the homogeneous suction.

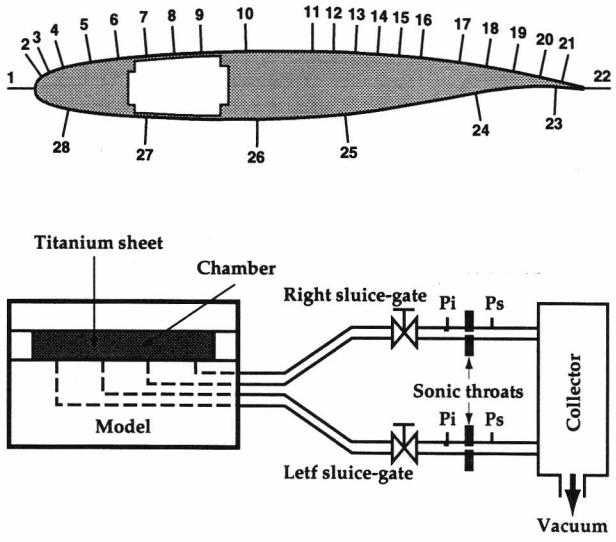


fig 4 : OALT25-B model and suction system

The boundary layer transition was fixed with carborundum grains at x/c=5% on upper and lower sides of the models for all tests with Reynolds number and suction variation. For tests with downstream displacement of the transition tripping, the transition was fixed on upper side with adhesive strip between 5% and 40% of chord and, on lower side, with carborundum grains at x/c=5%.

Instrumentation

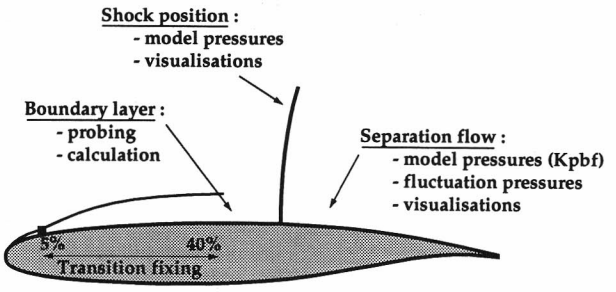


fig. 5 : Studied parameters

To analyse the chosen different parameters (figure 5), the following instrumentation is necessary.

- The cryogenic model, OALT25-A (figure 3), is equipped with 47 pressure taps to check the pressure distribution, with 47 thermocouples installed under the model skin to measure its temperature during the tests and with 6 unsteady pressure transducers installed at 40%, 50%, 60%, 70%, 80% and 85,7% .

The second model instrumentation, OALT25-B (figure 4), was totally adapted to the "suction" test. It is equipped with 28 pressure taps at the same chord position as the OALT25-A model, with 5 chamber pressure taps ("suction part") and with 4 unsteady pressure transducers installed at 70%, 80%, 85,7% and 90%.

- The boundary layer parameters were calculated by using total pressure probing (figure 6). It was performed upstream the shock position (54% of chord). The static pressure was supposed to be constant perpendicularly to the wall and measured by the model pressure taps.

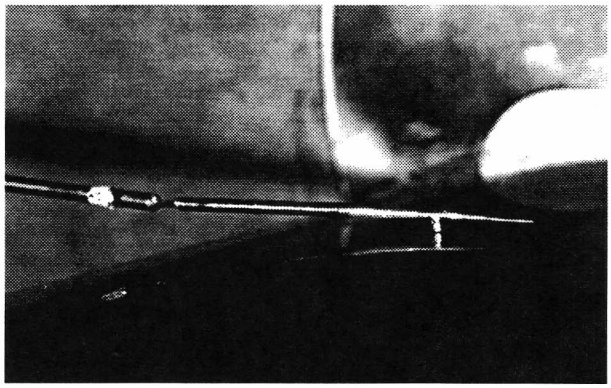

fig. 6 : Boundary layer pressure probing

- Surface oil visualisations, only used at ambient temperature, were performed to check the two-dimensional nature of the flow and to establish areas of separated flow. Mixing of oil and black powder (lamp black) or mixing of oil and white powder (titanium oxide) were used. A movie film was taken during the tests in order to better follow the surface flow direction.

Unsteady pressure transducers analysis

Each unsteady transducer was located near each static pressure hole. Records were obtained on magnetic tape for all tests. The data acquisition rate of the transducers is 2000 points / second. The spectra can be qualified in the frequency range between 0 and 1000 Hz.

Calculation of the boundary layer parameters

The velocity U(y) can be calculated from the probe measurements, Pi(y), by the following hypothesis : static pressure and total temperature are constant in the boundary layer. The determination of the wall location is performed by superposition of the average velocity profile and the logarithmic law of the surface turbulent zone. The parameters of the boundary

layer, $\delta 1$, $\delta 2$, Hi are deduced by formulas (cf. paragraph "Notation").

Calculations of two-dimensional compressible boundary layer (3) were made by using the local model Mach number measurements (static pressure taps). Boundary layer parameters versus x up to the shock position can be obtained, in particular just upstream the shock where the pressure probing is difficult to realise. The transition criterion uses the laminar instability theory and the "parabola method" (4).

## Tests conditions

The two models were mounted between the sidewalls of T2 transonic wind tunnel (fig. 7). Each test was performed by using self-adaptive top and bottom walls. All data presented in this paper correspond to adaptive cases obtained after an iterative process of 4 or 5 iterations.

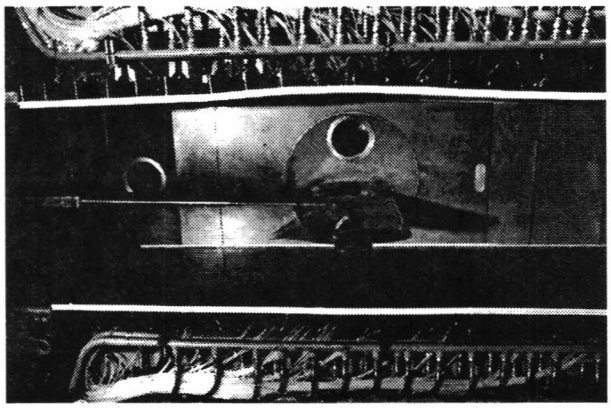

fig 7: Model in T2 wind tunnel

The Mach number range for this investigation was from M=0,72 to 0,80, the angle of attack range from $\alpha$=1° to 2,75° the Reynolds number range from Re=6 million to 20 million (pressure range from Pi=1,7 bar to 2,9 bars, temperature range from Ti=300K to 150K), the suction velocity range from Vasp=0m/s to 3,6m/s and the range of the transition tripping position from 5% to 40% of the model chord.

## Classification of shock/boundary layer interactions

A general classification of shock / boundary layer interaction and the corresponding excitation has been obtained by A. R. G. Mundell and D. G. Mabey (5). This is illustrated in fig. 8 for constant Mach number as the angle of incidence increases (2D).


(a) Weak shock thickens boundary layer

Excitation regions

1. Low level upstream of shock at all frequencies
2. Low level, low frequency, small scale close to shock
3. Tunnel-empty noise level (attached boundary layer pressure fluctuations outside measurement bandwidth)

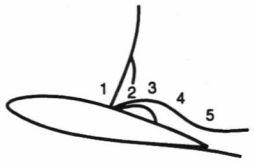


(b) Stronger shock locally separates boundary layer, followed by reattachment

1. Low level upstream of shock
2. High level, low frequency, larger scale fairly close to shock
3. High frequency due to bubble (outside measurement bandwidth in these tests)
4. Low frequency pressure fluctuations fall as boundary layer recovers after reattachment
5. Tunnel-empty noise level

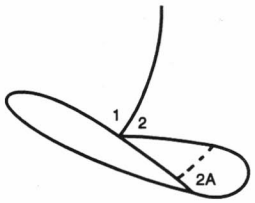


(c) Very strong shock separates boundary layer to trailing edge

1. Low level upstream of shock
2. High level, low frequency extends over wide region

2A. Towards the end of separated region high frequency pressure fluctuations from bubble appear in measurement bandwidth in these tests

fig. 8 : Classification of shock/boundary layer interactions and excitation on aerofoils.

Figure a sketches the interaction of a weak shock with a turbulent boundary layer. The main effect of the shock is to thicken the turbulent boundary layer. Three regions of excitation may be identified.

Figure b sketches the interaction of a shock sufficiently strong to separate the turbulent boundary layer locally, this separation being followed by reattachment. The main effect is a rapid increase in the boundary layer thickness at the trailing edge. Five regions of excitation may be identified. It can be different with other airfoils. A different type will be seen in the next paragraph. The trailing edge separation can appear before or at the same time as the shock separation.

Figure c sketches the final stage of shock induced separation. The strong shock waves induce boundary layer separation and no reattachment is observed on the airfoil. Three regions of excitation may be identified.

## Experimental results

### Test conditions

The figure 9 shows the increase in the trailing edge separation flow (trailing edge pressure coefficient, Kpbf) and the increase in the pressure fluctuation (RMS/Pi, x/c=85,7%) with the angle of attack increase and the Mach number increase (Re=6 million). The tests choice is to study only one Mach number, M=0,78 and to increase the angle of attack from 1° (no separation and very low pressure fluctuations) to 2,75° (separation and pressure fluctuations).

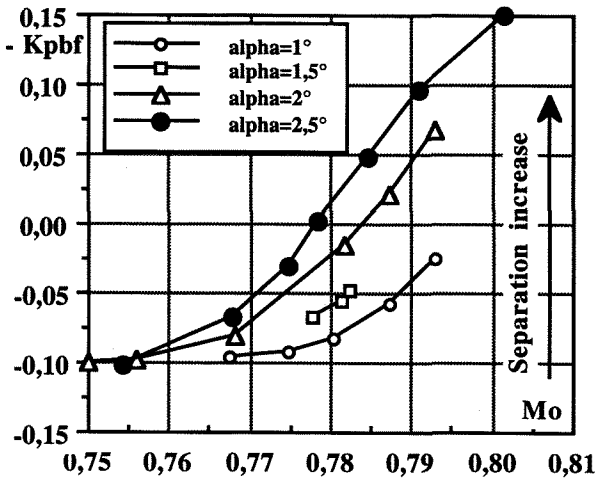


fig. 9a : Conditions test choice. Kpbf.

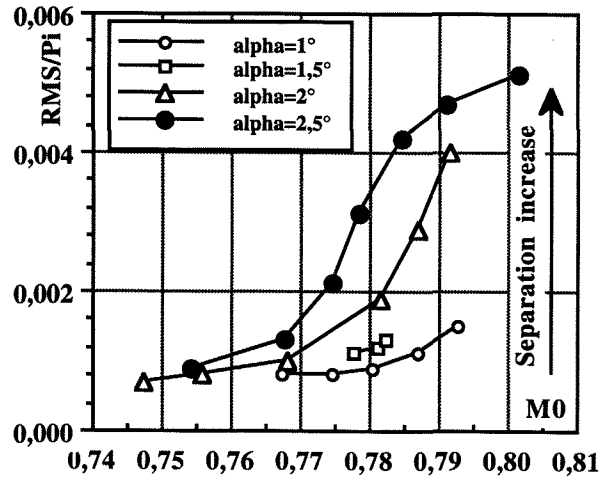


fig 9b : Conditions test choice.
Pressure fluctuations - RMS/Pi

Models comparison

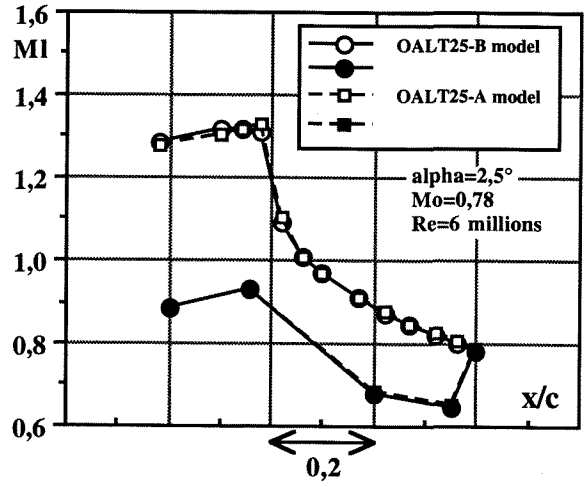


Fig. 10 : Models comparison

Local Mach number distributions of the two models, OALT25-A and OALT25-B, are presented in figure 10. Good comparative results can be observed. Comparisons between the different effects, Reynolds number, boundary layer suction and downstream displacement of the transition tripping can be made.

The OALT25 airfoil is laminar. The negative gradient upstream the shock can be observed (figure 10). That can stabilise the fluctuations.

Comparisons between boundary layer measurements (probing) and computations

Calculations of two-dimensional compressible boundary layer (3) can be realised with the local model Mach number measurements (static pressure taps).

The figure 11 shows the boundary layer displacement thickness, $\delta 1$, versus the suction velocity, Vasp. A good comparison between the measurements and the calculations can be observed. From the leading edge to the shock position, the calculated boundary layer parameters can be used, in particular just upstream of the shock.

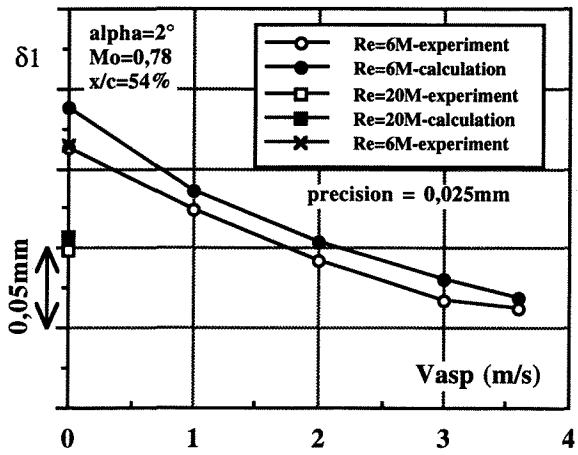


Fig. 11 : Displacement thickness comparisons

Comparisons of the Reynolds number effect, the boundary layer suction effect, the effect of the downstream displacement of the transition tripping

The evolution of the shock wave / boundary layer interaction and separation instabilities is analysed from the following parameters :

-boundary layer parameters,
-local Mach number distributions of the model,
-shock position,
-separation zones (oil flow visualisations, local pressure coefficient or Mach number distributions of the model and trailing edge pressure coefficients, Kpbf),
-unsteady wall pressure fluctuations.

- Boundary layer parameters

The figure 12 shows the evolution of the displacement thickness along the model chord for the following different test conditions.

| Test | Re (million) | Vasp (m/s) | x/cT (%) |
|---|---|---|---|
| 1 | 6 | 0 | 5 |
| 2 | 20 | 0 | 5 |
| 3 | 6 | 3,6 | 5 |
| 4 | 6 | 0 | 25 |

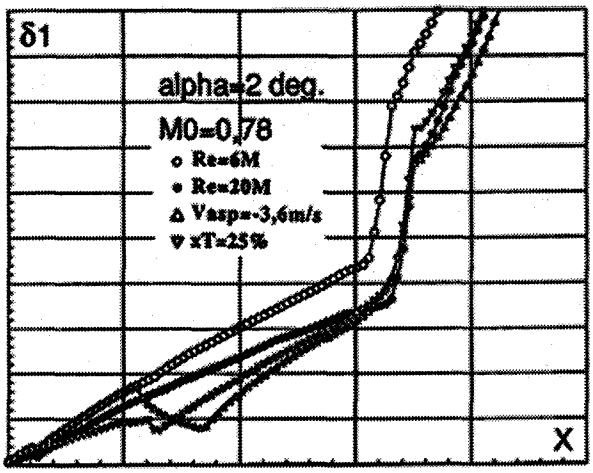


Fig. 12 : Displacement thickness versus chord

Different effects on the displacement thickness, δ1, can be observed. The decrease in δ1 when the Reynolds number increases, the abrupt decrease in δ1 where the suction is realised, the modifications of the curve with the position of the transition strip.

The figure 13 shows the evolution of the displacement thickness, δ1, versus the suction velocity, Vasp, and for Vasp=0m/s, for each Reynolds number and each position of the transition fixing.

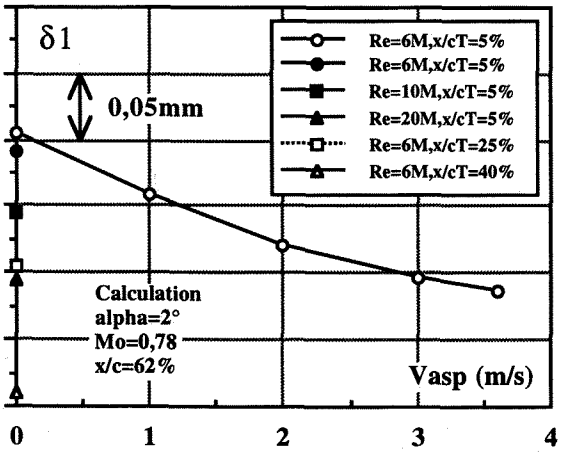


Fig. 13 : Displacement thickness versus suction velocity

Remarks can be made. The δ1 values decrease from the reference test, n° 1 (Re=6 million, Vasp=0m/s, x/cT=5%). They are similar just upstream of the shock position, x/c=62% (x=155mm), for the different test conditions 2, 3 and 4 (figures 12 and 13).

- Mach number distribution of the model

The figure 14 shows local Mach number distributions of the model for different test conditions.

General observations can be made. With the Reynolds number increase, or with suction velocity increase, or with downstream transition displacement, the shock position moves back and the flow separation decreases (observed on trailing edge pressure coefficient).

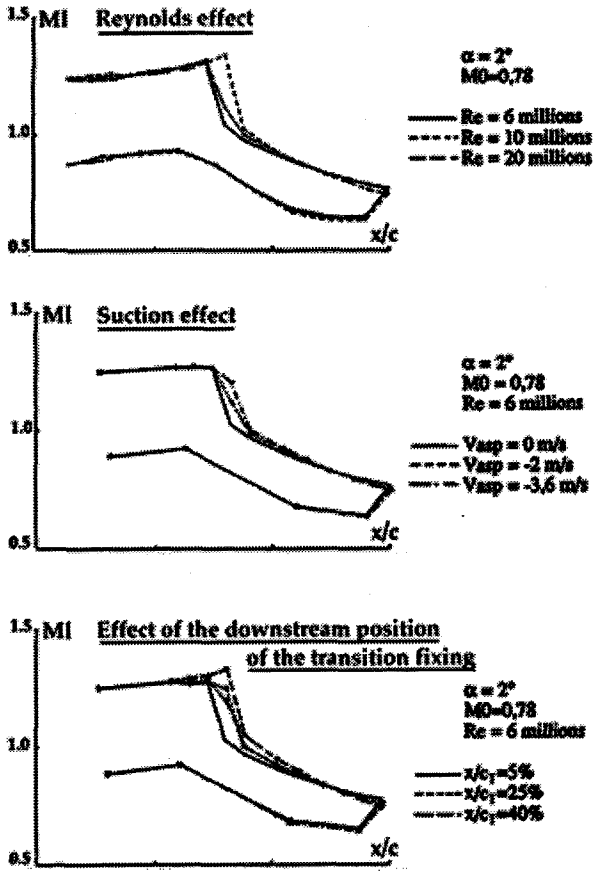


Fig. 14 : Mach number distribution

- Shock position evolution

The figure 15 shows shock positions for different test conditions. We can see that the shock position moves back with Reynolds number increase, suction speed increase and downstream transition position. The shock positions are about the same for the different test conditions 2, 3 and 4.

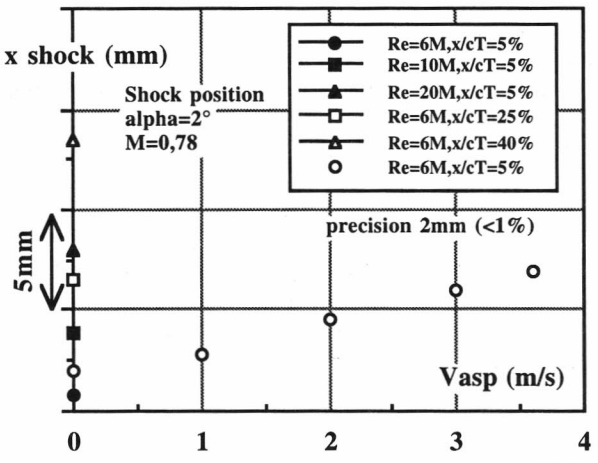


Fig. 15 : Shock position

We saw (figures 12, 13) that the displacement thickness values, $\delta 1$, were also the same just upstream the shock position (x/c=62%). It can be interesting to plot the shock position versus $\delta 1$ (figure 16).

The points are on the same line. The three different effects on the shock position are similar.

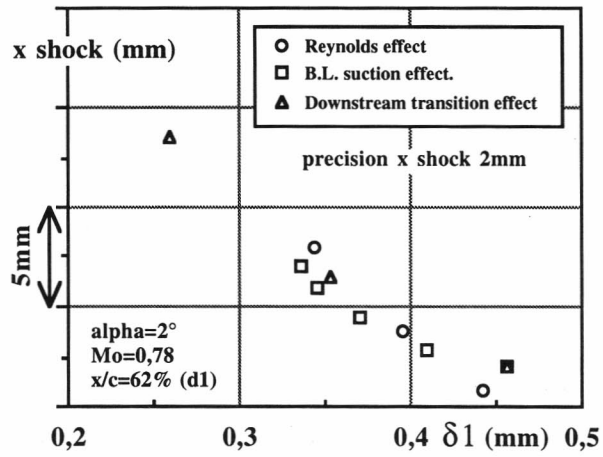


Fig. 16 : Shock position versus $\delta 1$

- Separation flow evolution

Surface oil visualisations were performed to establish areas of separation flow. Some pictures taken from the visualisations movie film are represented on figure 17. We can observe the different effects. The trailing edge flow separation zone decreases and moves back with Reynolds number increase and boundary layer suction. These two effects seem to be similar. No effect can be observed on the shock foot separation. The side walls effects induce the right and left vortex. The model centre must only be observed. No visualisation test was performed with the downstream position of the transition fixing.

Re=6M, Vasp=0m/s, x/cT=5%

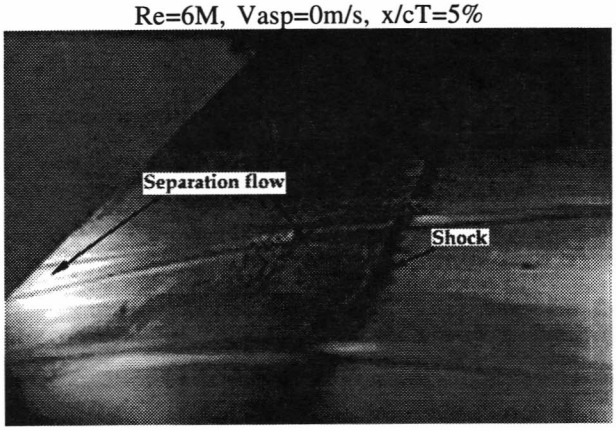


Re=10M, Vasp=0m/s, x/cT=5%

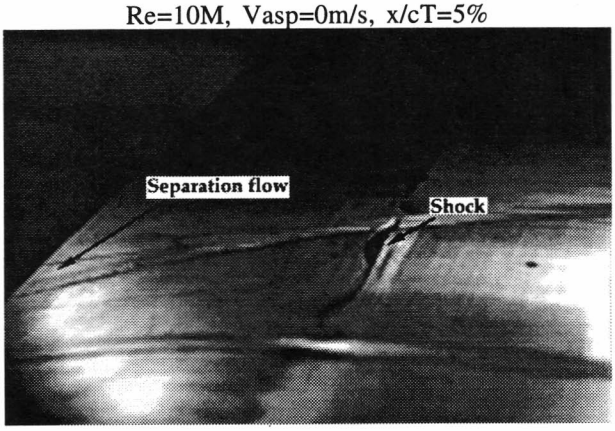


Fig. 17a : Separation flow evolution
Reynolds effect

Re=6M, Vasp=0m/s, x/cT=5%

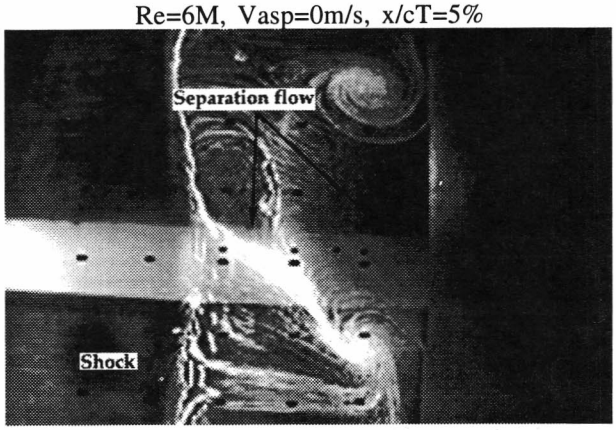


Re=6M, Vasp=1m/s, x/cT=5%

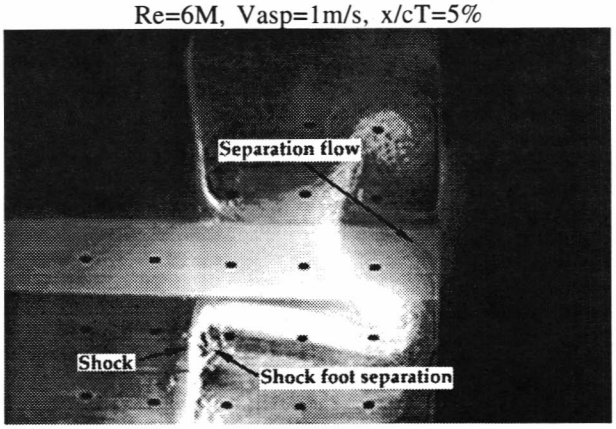

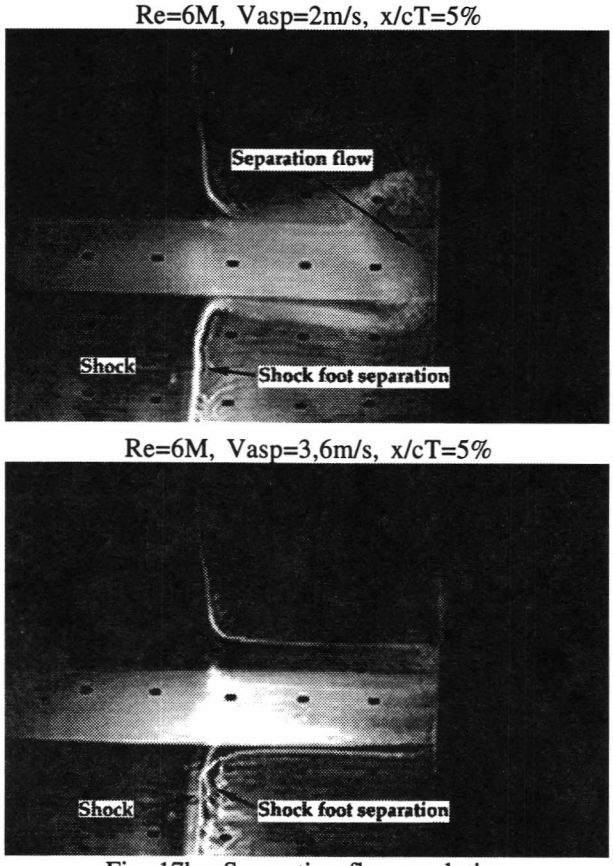


Fig. 17b : Separation flow evolution
Suction effect

The trailing edge pressure coefficient, Kpbf, can be a representative parameter of the trailing edge separation flow. The figures 18 and 19 show the Kpbf results with the three different effects.

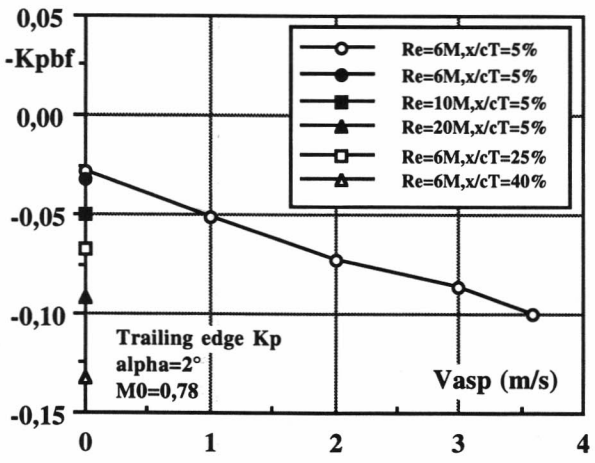


Fig. 18 : Separation flow
Kpbf evolution versus suction

We can see that the trailing edge separation flow decreases with the Reynolds number increase, the suction velocity increase and the downstream transition position (fig. 18). The trailing edge pressure coefficients are around the same for the different test conditions 2, 3 and 4. The figure 19 shows the trailing edge pressure coefficient, Kpbf, versus the boundary layer displacement thickness, $\delta 1$, calculated just upstream the shock position, x/c=62%. The points are on the same line. The three different effects on the separation flow are similar.

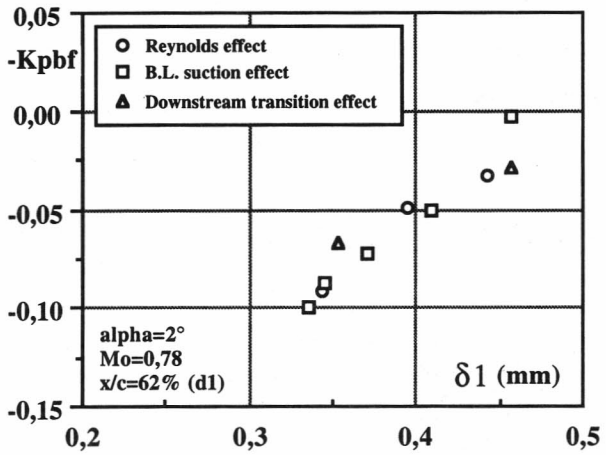


Fig. 19 : Separation flow
Kpbf evolution versus $\delta 1$

- Pressure fluctuations

The shock/boundary layer interaction can induce separation with instabilities. The ratio RMS/Pi can be a representative parameter of the pressure fluctuations or instabilities. The figures 20 shows the RMS/Pi results with the three different effects.

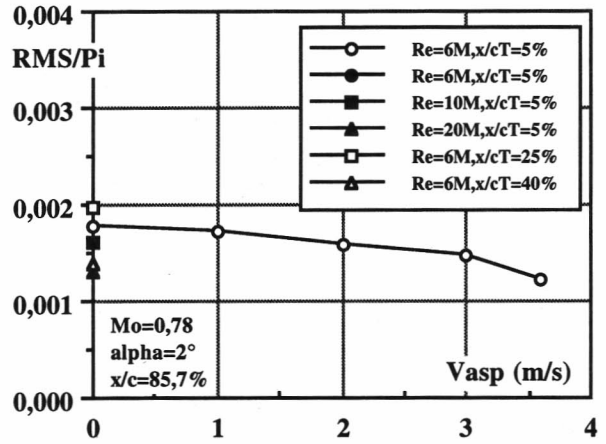


Fig. 20 : Pressure fluctuations
RMS/Pi evolution versus chord

The OALT25 airfoil is a laminar one. The fluctuation level is very low on this model. But, it can be possible to observe effects of the Reynolds number increase, the boundary layer suction and the downstream position of the transition fixing. The pressure fluctuations decrease, but not in the same proportion for the downstream position of the transition fixing. The x/cT=25% position is not sufficient to

obtain the same fluctuation level as Re=20M (test 2) and Vasp=3,6m/s (test 3). The x/cT=40% position is necessary. It seems to be difficult to have the same conclusion as with the last analysed parameters. But the differences between each test case are very small. We can say that the three effects are similar (figure 21).

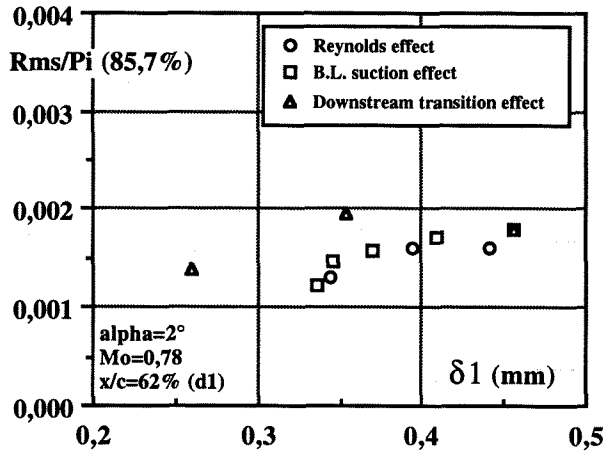


Fig. 21 : Pressure fluctuations
RMS/Pi evolution versus δ1

With the oil visualisations, the shock and trailing edge separation zones can be precisely determined.

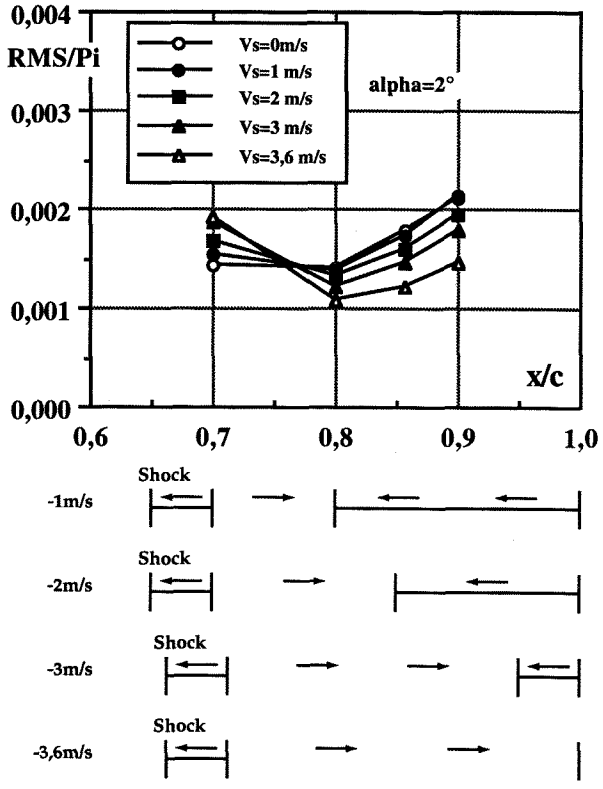


Fig. 22 : Pressure fluctuations
Transducers position/separation flow

The figure 22 shows the pressure fluctuations versus model chord. We can observe that the fluctuation level increases if the transducer is on a separation zone and that the fluctuation level decreases with the decrease area of the trailing edge separation flow. We can also observe that the boundary layer suction has no influence on the length of the shock foot separation zone.

A signal spectra analysis was performed. In order to be comparative, the 2,75° angle of incidence case producing larger instabilities was chosen (figure 23).

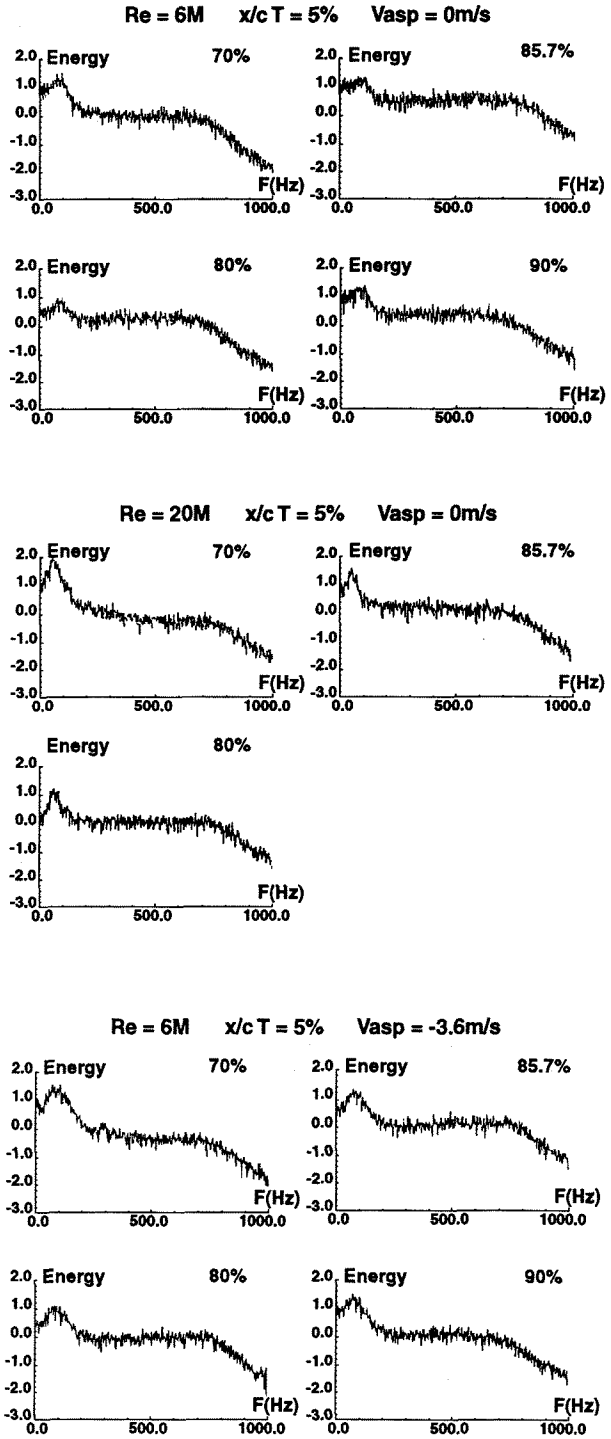

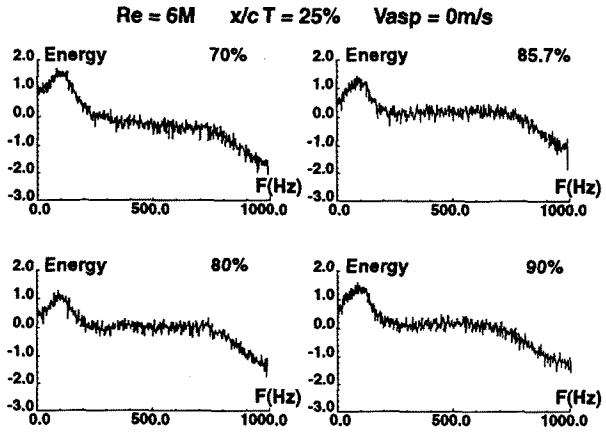


Fig. 23 : Pressure fluctuations
Spectra analysis

We can observe a frequency zone between 60 and 120 Hz with the high energy level. The tests at the Reynolds number of 20 millions were performed in cryogenic conditions (Ti=150K). The signal spectra analysis must be done with a reduced parameter, the Strouhal number :

$$n = \frac{f\,L}{U}$$

f :frequency

L : characteristic length (chord)

U : flow velocity

For each test case, the Mach number and the chord length are the same. But the velocity U is a function of the temperature, $U=a\,M=\sqrt{\gamma r T}\,M$ (for air, $\gamma$=1,4, r=287). Two unsteadiness flows are similar if they have the same reduced frequency $n=f1xL1/U1=f2xL2/U2$ so for this case, $f2=f1\sqrt{Ti1/Ti2}$.

For example, the results of the frequency with the high energy level for transducer at 85,7% of chord are shown in the following list. "fc" is the corrected frequency calculated at the ambient temperature.

| Test number | f (Hertz) | fc (Hertz) |
|---|---|---|
| 1 | 82 | **82** |
| 2 | 60 | **84** |
| 3 | 83 | **83** |
| 4 | 80 | **80** |

We can observe there is no big difference between the test case n° 1 (Re=6M, Vasp=0m/s, x/cT=5%), the test case n° 2 (Re=20M, Vasp=0m/s, x/cT=5%), the test case n° 3 (Re=6M, Vasp=3,6m/s, x/cT=5%) and the test case n° 4 (Re=6M, Vasp=0m/s, x/cT=25%). The higher energy frequency is more precisely marked for the test cases 2, 3 and 4. For these cases, there is no trailing edge separation. This frequency can be the fluctuation frequency of the shock foot separation. The three different effects on the frequency level of the instabilities are similar.

## Conclusion

These experimental studies have been performed on a laminar type airfoil to analyse the Reynolds number effect, the boundary layer suction effect and the downstream displacement effect of the transition tripping on appearance of unsteadiness resulting of shock wave / boundary layer interaction and flow separation.

The following parameters were analysed :

-boundary layer parameters,

-local Mach number distributions along the model,

-shock position,

-separation zones (oil flow visualisations, local pressure coefficient or Mach number distributions of the model and trailing edge pressure coefficients),

-unsteady wall pressure fluctuations.

These three effects decreased the boundary layer thickness, moved downstream the shock position, decreased the trailing edge separation zone, had no influence on the shock foot separation zone and decreased the unsteady wall pressure fluctuations.

Similar results were observed for these three different tests cases :

- Re = 20 millions, Vasp=0m/s, x/c transition = 5%
- Re = 6 millions, Vasp=3,6m/s, x/c transition = 5%
- Re = 6 millions, Vasp=0m/s, x/c transition = 25%

The Reynolds number effect, the boundary layer suction effect and the downstream position effect of the transition fixing on appearance of unsteadiness resulting from shock wave / boundary layer interaction and flow separation are similar. The displacement thickness, $\delta 1$, just upstream the shock position can be the mean parameter.

## References

1- Some instabilities arising from the interactions between shock waves and boundary layers.
N.C. Lambourne - Advisory Group for Aeronautical Research and Development.
Report 182 - April 1958

2- The Cryogenic Induction Tunnel T2 at Toulouse.
A. Séraudie - J.P. Archambaud - CERT ONERA
AGARD FDP/VKI Special Course - May 1996

3- CLIC - Calcul des couches limites compressibles.
B. Aupoix - D. Arnal - CERT ONERA
Rapport technique OA 23/5005 AYD - Octobre 1988

4- Transition prediction in transonic flow.
D. Arnal - CERT-ONERA
IUTAM Symposium Transsonicum 3 DFVLR-AVA Göttingen, 1988.

5- Pressure fluctuations caused by transonic shock/boundary layer interaction.
D.G. Mabey - A.R.G. Mandell.
Aeronautical Journal, August - September 1986